Wilhelm Roux's Archives 180, 121–147 (1976)

Roux's Archives of Developmental Biology


# Fibroblast Cultures and Dermatoglyphics: The Topology of Two Planar Patterns

Tom Elsdale and Frances Wasoff

Medical Research Council, Clinical and Population Cytogenetics Unit, Western General Hospital, Crewe Road, Edinburgh, EH4 2XU, 031-332-2471, Great Britain

**Summary.** This is a study of two, two dimensional biological patterns – the pattern created in a confluent dish of normal fibroblast and the dermatoglyphic pattern on the primate palm and sole. Both patterns are characterised by a small repertory of different types of interruptions or discontinuities in fields of otherwise parallel aligned elements. Because these discontinuities are invariant under plastic deformations as well as rigid motions, a topological treatment is appropriate. A quantitative topological characterisation shows the pattern in the two systems to be essentially identical. Regarding both systems as exercises in packing elongated elements in the plane subject to certain constraints, both can be modelled by a smooth, planar, non-oriented vector field. In neither case can the development of pattern be accounted for solely in terms of the aggregate of autonomously arising local detail; the whole constrains and influences the local situations. The interrelationship of global and local constraints on packing is quantified by the index theorem, which accounts for the range of patterns that may develop. The study shows that to understand pattern development in these systems, it is necessary to include topological considerations in addition to an analysis of cell behaviour.

**Key words:** Human – Morphogenesis – Pattern topology – Fibroblasts – Dermatoglyphics.

A close look at the structure of a dense culture of diploid fibroblasts reveals the elongated cells packed side by side in parallel arrays; ditches or discontinuities occur where arrays of cells with different orientations meet (Elsdale, 1968, 1973). These characteristic features of the pattern are large compared to the sizes of the individual cells (Elsdale, 1972). Thus a square large enough to include a typical discontinuity in the fibroblast array contains hundreds if not thousands of cells. Fields of this size are too large to be appreciated solely in terms of the interactions of the individual cells, the local form building activities in any small area are clearly subordinated to influences generated

over much larger areas. For this reason, an account of the morphogenesis of the fibroblast sheet as the resultant of individual cellular interactions, and hence as the aggregate of autonomously arising local detail, is bound to remain incomplete.

To complete the picture it is necessary to identify and quantify the influences from the whole and their local effects. This raises the problem of how to accomodate both local and global aspects of the form building processes within a single, comprehensive, and quantitative model of pattern development in this system.

The treatment we provide employs mathematics in the first place to quantify features of the pattern. We then show how a theorem in topology can be employed to quantify the reciprocal influence of the whole on local detail. To this extent mathematics is used as a tool to investigate the system. In an appendix the mathematics is presented somewhat more rigorously to develop a model.

The essence of the treatment is to regard pattern development as an exercise in packing elongated elements (the individual fibroblasts) in the plane, and to explore the constraints under which this packing occurs.

It turns out that it is necessary to refer to no more than rather general properties of the cells. This implies that our model may have more general application. With this in mind we have reinvestigated human dermatoglyphics. We discover that the loop, the whorl and the triradius are topologically the same as the discontinuities we observe in the fibroblast pattern. Topologically the two superficially different systems are identical and conform to the same model. There is a practical spin-off, for certain existing anomolies in dermatoglyphics are removed under the new treatment.

It appears therefore, that a topological approach reveals certain generalities underlying pattern development. It would be surprising if the methods and insights appropriate to two dimensional examples had no utility in the exploration of more complex situations.

## Material and Methods

Normal human diploid lung fibroblasts were obtained from 12–18 week foetuses. Cell lines were established in the routine way (Elsdale, 1968) and were maintained in F10 medium, with Hepes buffer 10% newborn calf serum, penicillin, streptomycin, and Fungizone. For this investigation. multilayering of the fibroblast sheet was inhibited by the addition of 20 μg/ml collagenase (Boehringer, Mannheim GmbH) to the routine medium. The main purpose of this study was to investigate the way in which densely packed cells organise. Cultures were therefore set up between $^2/_3$ and $1^1/_2\times$ confluence. Falcon plastic Petri dishes were employed throughout to avoid the introduction of an ordering pattern on cells, as we noted that other brands of dishes provided a biased substratum that influenced the alignment of the cells. To safeguard against setting up a cell density gradient, initial plating was carried out with the dishes placed on a flat, absolutely level, glass plate and the cell suspension poured with a minimum of turbulence; the initial plating density was seen to be uniform over the dish and cell orientation was random. Cultures were fixed at various intervals from one to ten days in a 1:4 solution of methanol and acetone at $-20°$ C and stained with May-Grunwald and Giemsa stains.

Cell movement and pattern simplification were studied with Wild time lapse cinemicrography apparatus.

Small bounded fields to constrain cell packing were made in two ways. Silicone grease was extruded from a syringe onto the floor of a petri dish in the desired shape for a boundary. There were either parallel grids of straight lines or circles. Smaller and more varied shapes were outlined by scratching boundaries with a sharpened pin. The diameters of the fields sketched in these ways ranged from one to ten millimetres.

## Packing Pattern in Fibroblast Cultures

*Development of the Closely Packed Monolayer.* We will first describe how the pattern of arrays and discontinuities characteristic of the confluent fibroblast cultures arises and evolves over time, before embarking on the mathematical description and analysis of the pattern. We describe the commonplace situation where a Petri dish culture is initiated at a pre-confluent density from a cell suspension.

The cells fall out of the medium and adhere to the substratum on which they extend randomly distributed and oriented. The cells move around and proliferate. The form of the cells, initially variable, becomes stabilised as confluence is approached, the cells adopting an uniform, elongated, bipolar spindle form (Elsdale and Bard, 1972). A tendency for the cells to adhere together side by side is evident before confluence, and these associations being more stable than other contacts eventually take over the culture. As a result the confluent culture consists of a patchwork of numerous independently formed parallel arrays. Where the cells in two adjacent arrays share the same orientation to within about 20° the arrays merge at confluence; where the orientations differ significantly, merging is inhibited and a discontinuity arises (Elsdale, 1972). Just as a culture reaches confluence, the appearance is confused, and there is a shake-down period of a day or so during which the culture accommodates to new close-packing requirements. The result is a tidy situation of arrays, in which the parallel alignment of neighbouring cells is precise, and clear discontinuities of characteristic form that appear as empty ditches between raised banks of cells (Fig. 1).

In the normal way, a three dimensional pattern of orthogonal multilayers forms in response to post-confluent growth (Elsdale and Bard, 1972), obscuring the two-dimensional pattern on the floor of the dish. We postpone a treatment of this important aspect of morphogenesis in fibroblast cultures, because different mathematics is required. Multilayering however can be inhibited altogether by adding small amounts of bacterial collagenase to the medium to prevent collagen accumulation. Under these circumstances all the cells produced by post-confluent growth are accommodated within the two-dimensional pattern we are interested in, the further evolution of which over time can be observed unobscured.

This evolution is a simplification of the pattern resulting from the elimination of discontinuities (Elsdale, 1972). Elimination is initially rapid but slows as the discontinuities become spaced further apart. The process depends crucially on the maintenance of conditions favouring high cellular mobility. Merging


**Fig. 1.** A dense patchwork of arrays of fibroblasts. The points of low cell density at the meeting of arrays are the discontinuities. These are of two distinct topological types (see text). Fixed preparation (16,2 ×)

of arrays is the concomitant of elimination. On prolonged maintenance, the number of discontinuities may reduce from many hundreds to a mere handful. There are topological reasons why not all the discontinuities can be eliminated. Simplification is irreversible.

*What to measure?* Interfaces are the essential ingredients of pattern. Thus the nerve tube, notochord, and somites in a cross section through an amphibian neurula are distinguished by the interfaces between them (Hamilton, 1969); without these discontinuities there would be no embryonic axis, merely a formless condensation of otherwise indistinguishable cells. A field of fibroblasts in uninterrupted parallel array is a bland and featureless continuum; it is the discontinuities that are the distinctive ingredients of the packing pattern, and it is these that we are concerned with.

Even though a fibroblast culture exhibits only an elementary kind of mophogenesis, the details of packing, and pattern simplification reveal a high degree of order (Elsdale, 1973). There are restrictions on the form of discontinuities and the excess number of one type over another that yield to a geometrical analysis. Using appropriate mathematics, precise quantitative measurements can be made, and quantitative theorems brought to bear; for this reason a treatment that is more than a mere description can be provided carrying important insights into the nature of the system.

*Characterisation of Discontinuities by their Topological Index.* Although a discontinuity can be seen to have a certain shape or form, the mathematical characterization does not take account of this form directly. Instead, it takes account of the way the cells are arranged in the immediately surrounding field.

Consider by way of introduction a field of cells in uninterrupted parallel array. Mark a point anywhere within this field, and draw a circle about it. Note the orientation of each cell encountered in the course of a tour around the circle. Obiously, in this case, the orientations are the same. We allude to this fact by saying that there is no rotation of the field elements about arbitrary points in the field. This is the mathematical way of observing that a parallel array is a bland continuum.

The situation around a discontinuity will be different. Here a rotation of the field elements is always observed. Thus to characterise a discontinuity we characterise the rotation of the field (elements) in its neighbourhood. We need to do two things; firstly, measure the amount of rotation, and secondly, determine the sense or direction of the rotation along the lines of finding out whether a screw has a left hand or right hand thread. These two items of information are expressed in the *Topological Index* (Lefschetz, 1957; Petrovski, 1966). This index, the basic measurement used in this treatment, is thus a composite parameter, it consists of a figure giving the amount of rotation, preceded by a sign $+$ or $-$ which distinguishes which of two senses the rotation takes.

A rotation of 360° or $2\pi$ radians (think of the radiating spokes of a cycle wheel) is counted as 1, and a rotation of 180° or $\pi$ radians as $^1/_2$. How to compute indices, the use of the sign convention, together with a brief topological

analysis of the index is presented in the section of the appendix entitled computation of the index. For brevities sake, we shall often refer to a "+1" or a "$+^1/_2$" discontinuity; bear in mind however that the index, properly speaking, is a measurement made on the surrounding field.

The index has a particularly important and valuable property. Figure 2b for example, shows a typical three armed $-^1/_2$ discontinuity. Examples of this discontinuity are often symmetrical, each arm lying at an angle of 120° to the other two. Sometimes the arms are not symmetrically disposed. It does not matter. Computation on drawn figures will show that the computed index is the same (Fig. 3). Thus all point discontinuities at the confluence of three arrays compute to the same index, $-^1/_2$, allowing for trivial measuring errors. Another way of alluding to the same property is to note that the index remains unaltered where a discontinuity is subjected to small perturbations that do not destroy the underlying topology. In fact discontinuities are continually subjected to small perturbations, for fibroblasts are motile and individual cells move in and out of the immediate neighbourhood of a discontinuity.

*Discontinuities Observed in the Packing Pattern.* Bearing in mind how a culture grows to confluence, by the expansion and eventual merging or interdigitation of independent arrays, it might be thought that discontinuities would arise with a wide range of associated indices. In fact the pattern that emerges after confluence and shakedown reveals only two forms: discontinuities with associated indices of $+^1/_2$, and $-^1/_2$ (Fig. 2a, b). Furthermore, these are the simplest forms; the $+^1/_2$ arises at the confluence of two arrays, the $-^1/_2$ at the confluence of three arrays.

These are not, of course, the only theoretical possibilities. We find two additional discontinuities during the shakedown period. They have indices +1 and −1 (Fig. 2c, d). These and all other discontinuities whose index is an integral multiple of $^1/_2$ share the common property of decomposability. This is manifested in the fibroblast culture by instability (Elsdale, 1973). Thus the influx of cells along any diameter of a +1 discontinuity results in the separation of two $+^1/_2$ discontinuities. (Fig. 4a). The −1 is unstable along either one of the two planes of slippage and two $-^1/_2$s separate (Fig. 4b). The instability of the −1 is also observed on the surface froth of soap bubbles assuming hexagonal packing.

Notice that all the discontinuities observed in fibroblast cultures have indices of a $^1/_2$ or integral multiples thereof. This represents a very important restriction and allows the adoption of the mathematical model given in the appendix. These discontinuities, and these alone, share the property that the fields in their neigh-

**Fig. 2. a** A discontinuity of topological index $+^1/_2$. This is one of the two stable types of discontinuity found in mature fibroblast monolayers. Fixed preparation (36×). **b** A discontinuity of index $-^1/_2$, the other stable discontinuity arising at the meeting of three arrays. Fixed preparation (×100). **c** This discontinuity has index +1. It is an unstable form arising as cultures approach confluence; through cell movement it decomposes into two $+^1/_2$ discontinuities. Fixed preparation (×150). **d** This discontinuity, whose index is −1, is also unstable. It will decompose into two $-^1/_2$ discontinuities through movement along one of its two planes of slippage. Living cell under phase contrast (×130)

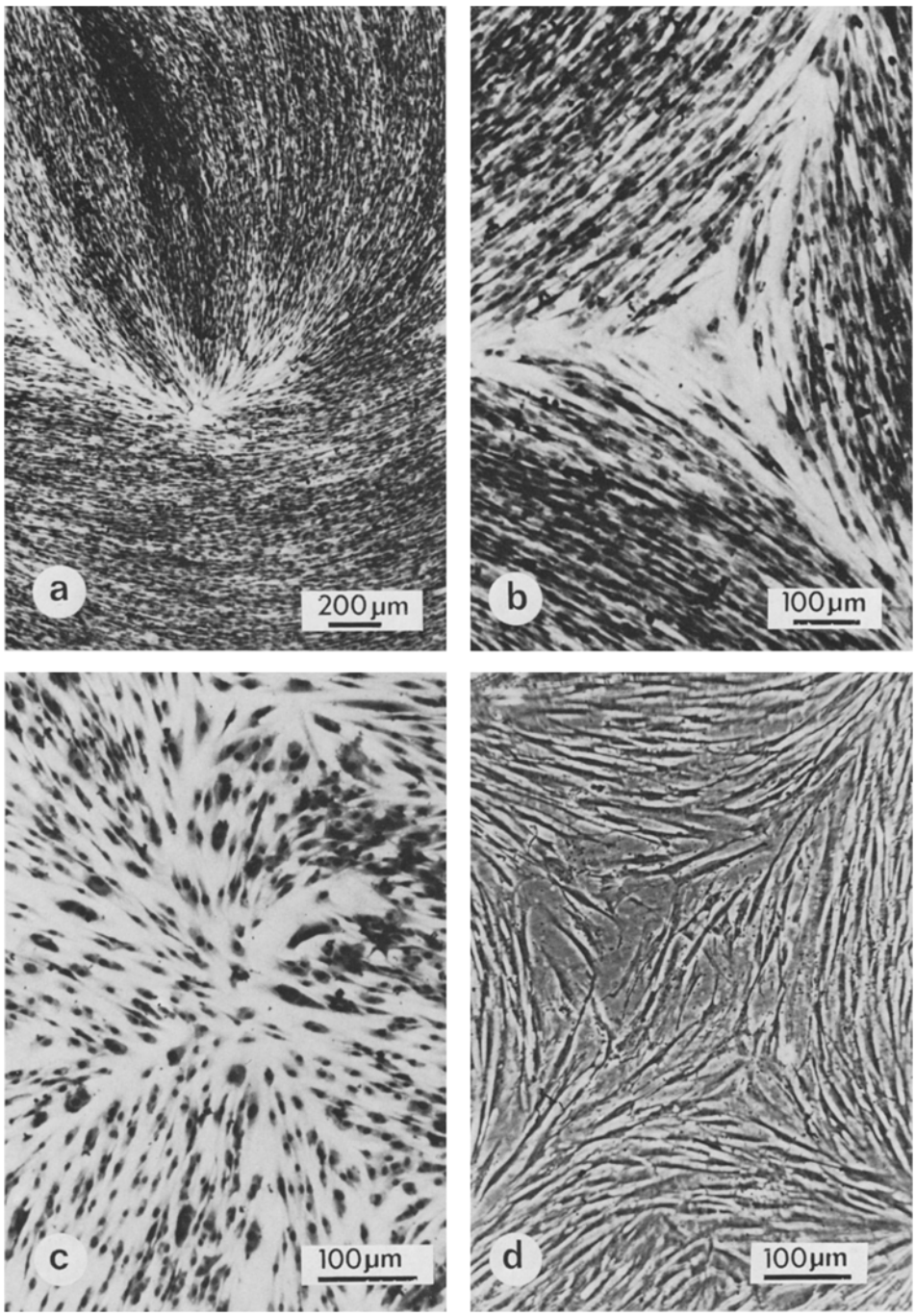
a
200 µm
b
100 µm
c
100 µm
d
100 µm

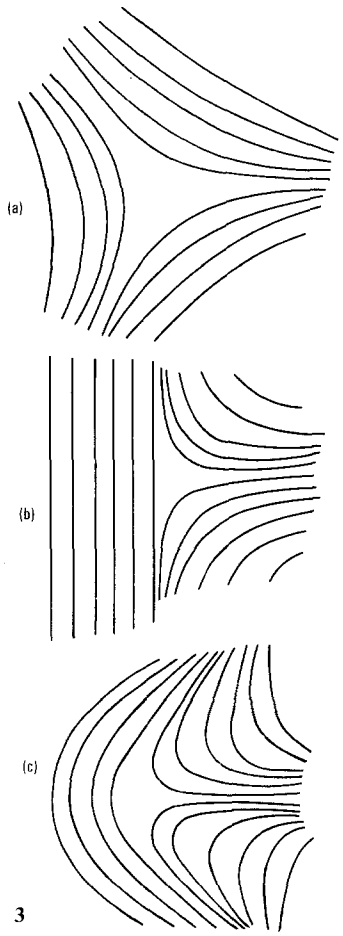


Fig. 3a–c. See text

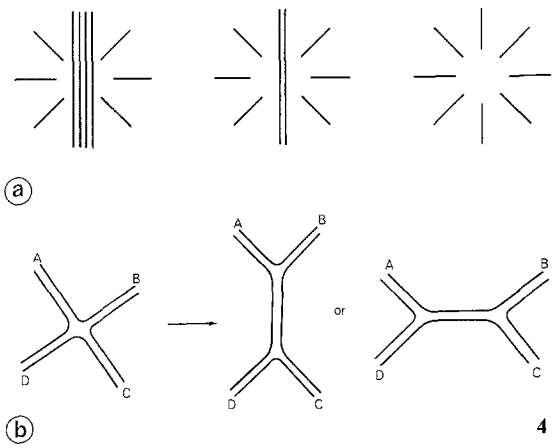


Fig. 4a–b. See text

bourhood are everywhere characterised by smooth change. Adjacent cells are everywhere similarly oriented. Discontinuities of other indices are readily drawn on paper, but in all cases the tour around the circle will reveal one or more locations where adjacent elements point in sharply different directions.

Two conclusions are drawn from these observations:

1. Fibroblast fields are characterised by smooth change around point discontinuities.

2. $+^1/_2$ and $-^1/_2$ discontinuities, alone observed after the shakedown, are the only two non-decomposable discontinuities possible under the restriction imposed by 1.

*The Elimination of Discontinuities.* The rotation associated with a discontinuity is an established feature of the fibroblast field, and cannot disappear by itself.

A discontinuity can become effaced on the field boundary (with a concomitant change of the boundary index, see later), but as the process of elimination already referred to, takes place as well in the middle as the periphery of a dish, there must exist another more general mechanism responsible for simplification.

Because the cells are continually moving around, discontinuities are, to a limited extent motile, bear in mind however that this is a mere figure of speech —only the cells do the moving. As a result of this "motility" discontinuities can approach one another. The mutual approach of $+^1/_2$ and a $-^1/_2$ creates a situation that allows for their mutual elimination. We have watched these mutual eliminations, they occur as in Figure 5. Mutual elimination reflects the additive nature of rotations. Under appropriate circiumstances a rotation in one sense can cancel the same amount of rotation in the opposite sense:

$$(+^1/_2)+(-^1/_2)\rightarrow 0.$$

This mechanism is stochastic and depends on the random encounters of discontinuities of unlike sign. The process slows rapidly as discontinuities become sparse, analogous to concentration dependent kinetics.

Notice that in the equation above a unidirectional arrow is employed, not an equal sign. This follows because a change in the reverse direction is never observed and, would indeed be a discontinuous change if it did, contradicting our previous conclusion that fibroblast fields are characterised by smooth change.

We draw two further conclusions:

3. Simplification occurs as the result of mutual eliminating interactions between pairs of discontinuities of unlike sign.

4. The irreversibility of simplification is a consequence of the smooth nature of the fibroblast field.

*Restrictions on Packing Within Bounded Fields: The Index Theorem.* There is more "structure" in a fibroblast field than the foregoing considerations bring out. There are restrictions on the balance of discontinuities of different sign related to the alignments of cells at the boundary of the field. The required intuition here is that the balance of positive and negative rotations within a finite field will dictate the alignments at the boundary, and conversely, a particular boundary alignment is consistent with a particular balance of positive and negative rotations within the field.

As motivation consider the two simple situations below (Fig. 6).

Figure 6a is the simplest situation that arises where fibroblasts are plated over an open rectangle consisting of two parallel scratches on the floor of a plastic dish. Cells extend preferentially along the scratches, and in this simplest case the space between is packed by a single array. Consider now the alignments at the boundary of the subfield defined by the dotted rectangle. On the sides marked A the cells align tangentially at the boundary, on the sides marked B radially to the boundary. There are two A regions and two B regions; the

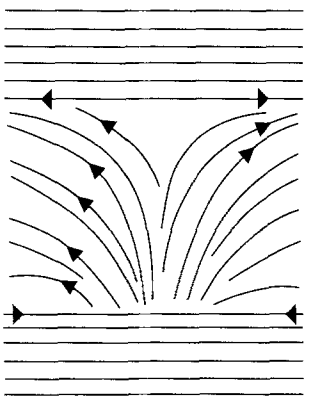

5

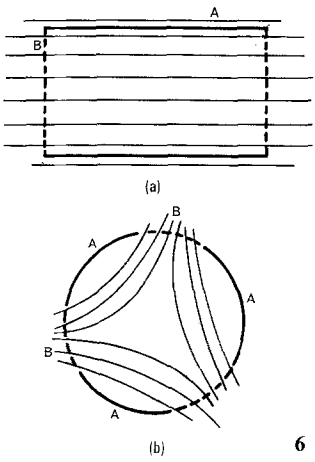


6

**Fig. 5.** Mutual Elimination of discontinuities. Cells move to and from the discontinuities along the paths sketched. The lower horizontal array moves closer to the upper one as the intermediate cells migrate out, resulting in a single parallel array

**Fig. 6.** See text

A regions alternate with the B regions. We term this a boundary with two gates. It is obvious that any finite field in uninterrupted parallel array will have a two gated boundary (Fig. 8a), and any subfield in parallel array, part of a larger and more complex field, can have an arbitrary 2 gated boundary defined on it.

Figure 6b shows a simple situation that arises where fibroblasts are plated onto a scratch pattern essentially a circle with three openings. The cells align against the scratches as before and the open regions of the circle tend to be colonised as shown in the figure. The field cannot be filled by a single array as before, at least one discontinuity is obligatory under close packing. The simplest case is a single $-1/2$ discontinuity as shown. The boundary marked by the dotted line here has three A regions alternating with three B regions, hence three gates. It is obvious that every subfield enclosing just a single $-1/2$ discontinuity will possess a three gated boundary (Fig. 7c).

These considerations reveal an alternative way of characterising discontinuities (and their absence) in terms of the number of gates on arbitrary subfield boundaries enclosing them. We have illustrated how a two gated boundary is associated with a zero rotation and a three gated boundary with $-1/2$ rotation.

The next step, having recognised that the number of gates on the boundary and the enclosed disconinuity are both reflections of the same rotation of the field, is to associate the topological index with both. Thus a two gated boundary has index 0 and a three gated boundary index $-1/2$. Although arrived at from a consideration of the situation around single discontinuities or their absence, this characterisation in terms of the index, will remain valid, wherever such boundaries occur, or can be arbitrally defined, and regardless of the number of discontinuities enclosed.

In the appendix indices of boundaries with different numbers of gates are computed directly from first principles without reference to enclosed discontinuities, and it is shown how each additional gate reduces the boundary index by $^1/_2$. From this the following series emerges:

| Number of gates: | 0 | 1 | 2 | 3 | 4 | 5 | 6 ..... |
|---|---|---|---|---|---|---|---|
| Boundary index: | $+1$ | $+^1/_2$ | 0 | $-^1/_2$ | $-1$ | $-1^1/_2$ | $-2$ ..... |

Where only $+^1/_2$ and $-^1/_2$ discontinuities are permitted it is obvious that in the case of a boundary without gates the simplest field must contain more than one discontinuity – two $+^1/_2$ s in fact. Similarly, a four gated boundary cannot enclose less than two $-^1/_2$ discontinuities, and a six gated boundary less than four under close packing.

This shows in principle how the boundary index can reflect, in a quantitative way, packing in fields containing more than one discontinuity. Indeed a quantitative relation exists no matter how many discontinuities are present.

This relation can now be stated in its general form.

Index Theorem: The index of the boundary = the sum of the indices of the enclosed discontinuities.

This theorem is a basic result in topology and of fundamental importance in our treatment of packing.

Three implications of the theorem are to be noted:

1. Consider, by way of example, fields of boundary index $+1$, and assume $+^1/_2$ and $-^1/_2$ discontinuities only. The theorem implies: – No field can contain an uninterrupted parallel array (no discontinuity), nor, only a single discontinuity. The simplest field contains two $+^1/_2$ discontinuities. Fields containing three discontinuities are impossible, and by extension so are all fields containing an odd number of discontinuities. Fields containing four, and by extension, any higher even number of discontinuities are possible, provided that for each $-^1/_2$ introduced a complementary $+^1/_2$ is also introduced so that the sum of the indices remains $+1$.

2. We found earlier, for example, that every field in uninterrupted parallel array has a two-gated boundary. Clearly the converse need not be true; the index theorem, however, adds the proviso that after all possible pairwise eliminations, the converse will be true.

3. Note the dual nature of the index theorem. Where pattern first constitutes a boundary and spreads inwards to fill the enclosed field, the index of the boundary dictates the sum of the indices of the discontinuities within. Where, on the other hand, a pattern is established that spreads outwards from a centre to cover a bounded surface, the sum of the discontinuities dictates the alignments at the boundary.

*Fibroblast Packing Exemplifies the Index Theorem.* Fibroblasts were persuaded to form small fields of different boundary indices. Prepared Petri dishes were employed bearing annular patterns of radial and tangential scratches. The field size was chosen to accommodate a small and manageable number of discontin-

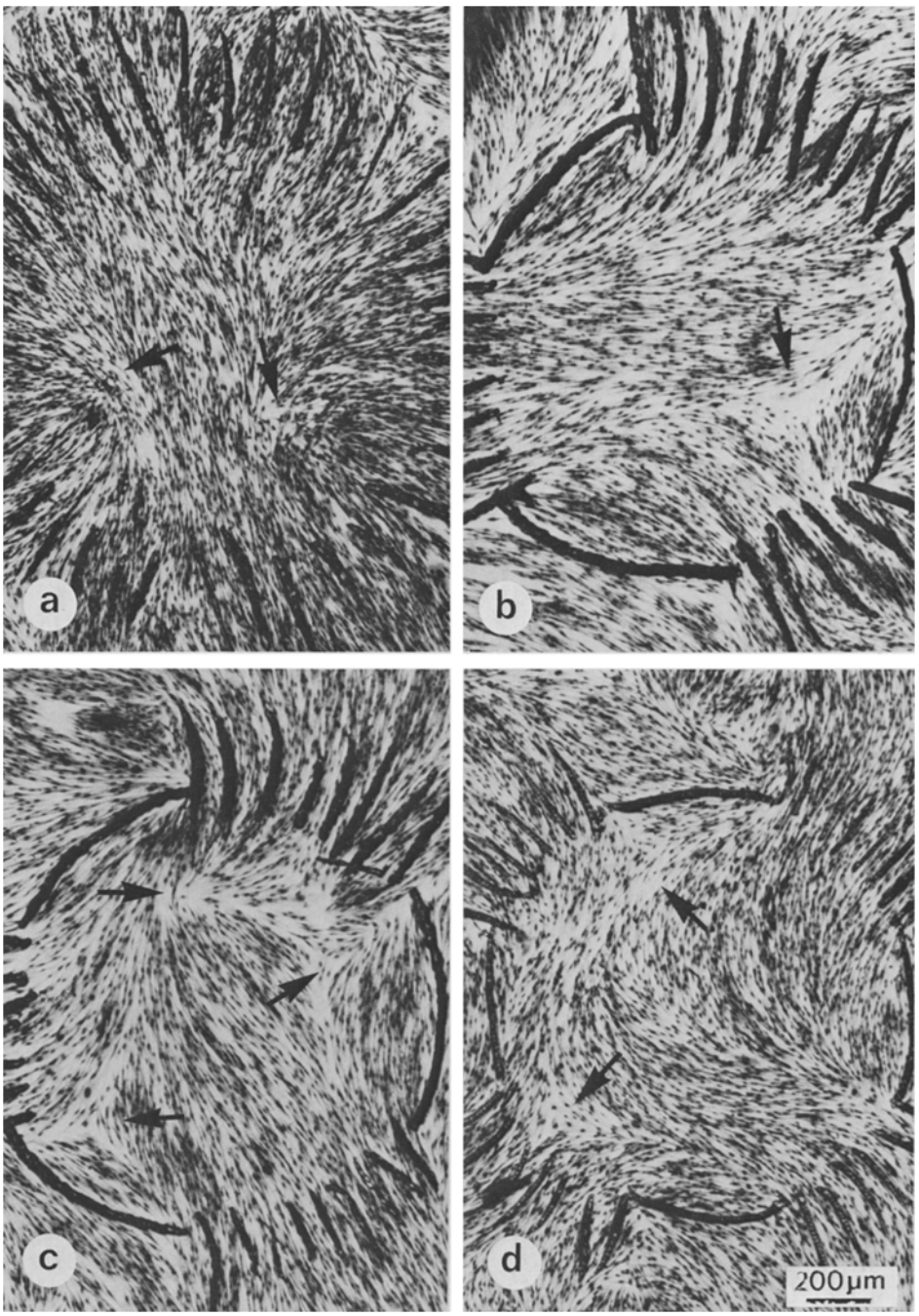


**Fig. 7a–d.** Small bounded fields of varying boundary index, illustrating cell packing pattern as a consequence of the index theorem. Notice that cells align along scratches. Fixed preparations (×50). *A* Boundary index +1: minimal number of discontinuities, 2× ($+^1/_2$). *B* Boundary index $-^1/_2$: minimal number of discontinuities. There is a single branch point. *C* Boundary index $-^1/_2$: there is an extra pair of discontinuities of opposite type. *D* Boundary index −1: minimal number of discontinuities $2\times(-^1/_2)$

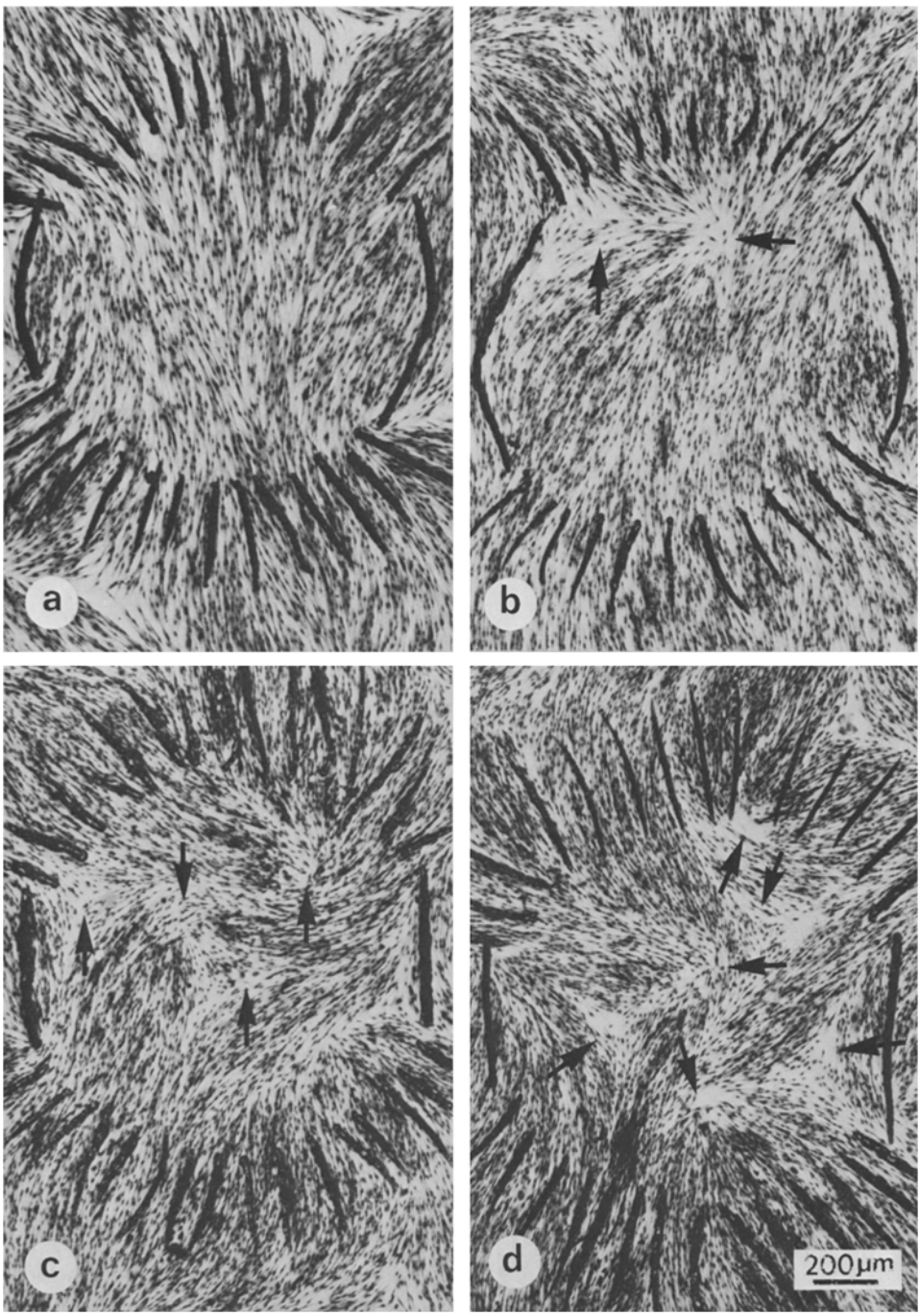


**Fig. 8a–d.** The boundary index of all of these small bounded fields is zero. Notice that the index theorem *does not* predict the absolute number of discontinuities nor their location. Fixed preparations (×95). **a** A single parallel array is packed into the field. **b** One extra pair of discontinuities their sum equals zero. **c** Two extra pairs of discontinuities. **d** Three extra pairs of discontinuities

uities. 50 mm. dishes containing up to 18 well separated scratch rings were seeded with near confluent innocula of cells. Cultures were maintained with medium changes for up to two weeks, in the presence of collagenase to inhibit multilayering, prior to fixation and staining to provide permanent preparations for examination and photography. We have examined several hundred fields of indices ranging from $+1$ to $-2$ containing up to fourteen discontinuities.

In scoring these cultures a crucial factor is how the cells align in the region of the boundary templates. The scratches persuade rather than coerce, and it was necessary in every case to ascertain the index of the boundary actually formed by the cells. It is important also to recognise that the boundary made by the cells is somewhat different from the scratch pattern insofar as the latter consists of abrupt alternations of groups of radial and tangential lines, whereas the cells negotiate the alternations smoothly (Fig. 19). The boundary index ascertained, this was compared with the sum of the indices within, derived from scoring discontinuities. Representative fields are shown in (Figures 7 and 8). We conclude that fibroblast packing exemplifies the index theorem.

## Dermatoglyphics

*Characterisation of Discontinuities.* The palmar surface of the primate hand and the plantar surface of the foot consist of closely-packed non-overlapping elongated elements; the dermal ridges (Cummins and Midlo, 1961). The pattern is essentially two dimensional. We shall show that this system provides a further illustration of pattern formation by elongated units subject only to packing necessities and boundary constraints. We are not concerned here with the fine details of the pattern used for purposes of individual identification; only in the features that are invariant through growth.

Over most of the palmar surface the epidermal ridges run parallel to one another. Within the body of the hand four types of interruption or discontinuities are recognised: the arch, the loop, the whorl, and the triradius (Fig. 9a). The arch is not a proper interruption, merely a rippling in the array; no rotation of the field is associated with it, it will not be considered further. The loop and the whorl are related; two loops put together make a whorl. The triradius is clearly different.

The triradius, with index $-{}^1/_2$ is immediately recognisable from its occurrence in fibroblast cultures. The loop and the whorl look superficially different from the forms we have met, but appearances can be deceptive. The relationship between the fibroblast and dermatoglyphic forms is revealed in the following figure. In Fig. 10 the $+1$ and $+{}^1/_2$ fibroblast forms are drawn in heavy lines. Superimposed on them is a system of thinner lines everywhere perpendicular to those beneath. The new figures so produced are the whorl and the loop. (For completeness, try the same with the triradius.) Restated mathematically, the fibroblast and dermatoglyphic forms are related by orthogonal transformation. This transformation, because it does not alter topological relationships, leaves the topological index unchanged.

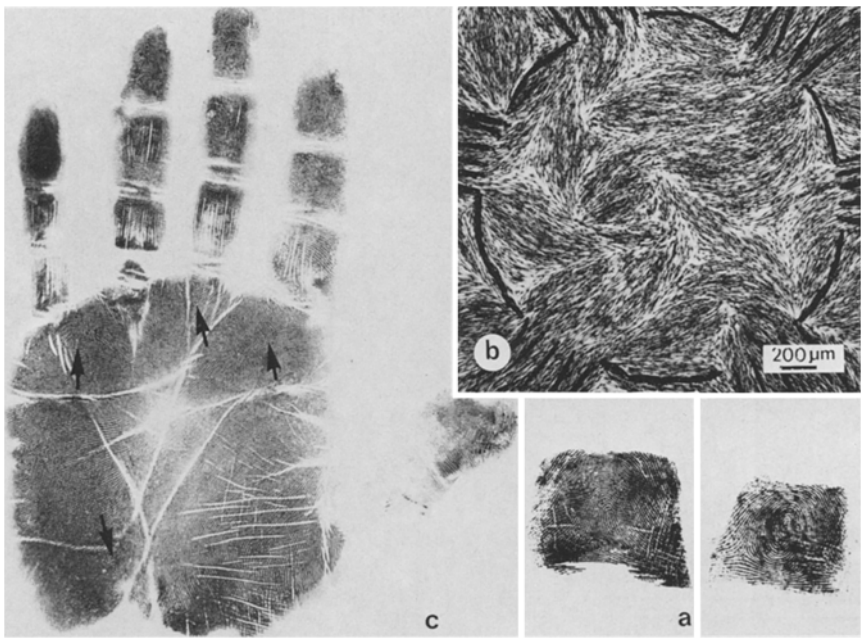


**Fig. 9. a** The patterns found in dermatoglyphics−, loop, whorl, triradius. Notice the ridge alignment at the edge of all of these fingertips are essentially alike; they all form fields whose boundary index is zero, and therefore indices of all the discontinuities sum to zero. **b** The handprint pattern is a further example of the Index Theorem. Tangential ridge alignment at the fingertips and wrist and nowhere else give a boundary index of −2. Hence the index therorem predicts the four excess triradii (see text). **c** A sic gated fibroblast field. There is a relative excess of four ($-{}^1/_2$) discontinuities over the ($+{}^1/_2$) discontinuities. Fixed preparation (×35)

Conclusion: Fibroblast patterns and dermatoglyphic patterns share the same topology.

*Penrose' Rule and the Index Theorem.* The formal identity just noted raises the question whether the same boundary constraints that structure the fibroblast pattern, also structure the dermatoglyphic pattern. An excess of triradii over loops and whorls, and the relation of this excess to gross features of the hand was formalised by L.S. Penrose (Penrose, 1965). He was primarily concerned with the use of dermatoglyphic data in clinical diagnosis, and it was useful to have a quick way of checking that all the characters on a hand had been counted and none overlooked. From an empirical study of normal, congenitally malformed, and non-human primate hands and feet, he arrived at the following universal rule.

Penrose' Rule: The number of triradii plus one = The number of loops plus the number of digits.

or, $T+1=L+D$ (1 whorl = 2 loops).

The rule implies that the number of excess triradii is always one less than the number of digits.

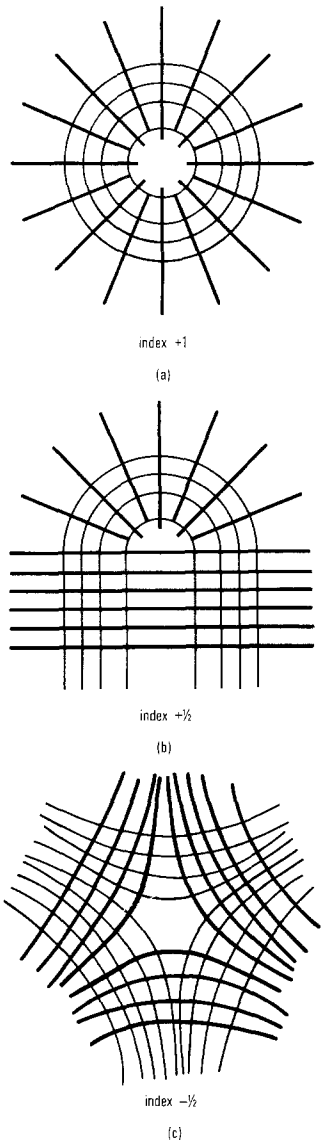


**Fig. 10a–c.** Orthogonal transformation (see text)

Is Penrose' Rule a special statement of the index theorem? To approach this question it is first necessary to measure the topological index associated with the boundary of the dermatoglyphic field. Take the normal hand. Inspection shows that at the periphery of the dermatoglyphic field the dermal ridges run predominantly radially or tangentially. At the wrist and over the ends of each digit, the ridges run tangentially; elsewhere, up the sides of the palm and the sides of each digit, the dermal ridges run radially (Fig. 9c). It is a nice coincidence that the treatment in terms of gates already used, and evolved in connection

with artificial boundaries, should be uniquely appropriate to this in vivo boundary. The normal hand has six gates. From the number of gates, the boundary index can be computed: Index $= 1 - {}^1/_2$ (number of gates). The boundary index of the normal hand $= -2$.

With this information the index theorem may now be applied. The sum of the indices of the discontinuities within the dermatoglyphic field $= -2$. This implies four excess triradii over loops and whorls (counting a whorl as 2 loops). This is the same result as given by Penrose' Rule.

Penrose' Rule further states that in the case of malformed hands, the number of excess triradii is one less than the number of digits. In terms of the index therorem: if there are D digits, the boundary of the dermatoglyphic field will show $D+1$ gates (the wrist, remember, adds one). The index therorem equates the sum of the indices of the discontinuities within the field with the figure $1-{}^1/_2$ (number of gates). If T represents tht total number of triradii and L the total number of loops and whorls, the sum of their indices will be ${}^1/_2 L - {}^1/_2 T$. The index theorem therefore states:

$$({}^1/_2 L - {}^1/_2 T) = (1 - {}^1/_2 (D+1)).$$

Simple arithematic shown that this is equivalent to:

$$T - L = D - 1$$

where the left hand side represents the number of excess triradii.

By a simple rearrangement we arrive at Penrose' original formulation:

$$T + 1 = L + D.$$

We thus demonstrate that Penrose' Rule is a special statement of the Index Theorem.

*Implications of Index Theorem and Removal of Anomalies.* There are practical advantages to using the index theorem in preference to Penrose' Rule. First the Index theorem is more general in its application for unlike Penrose' Rule it can be applied to any portion of the hand. For example, consider the situation on the distal phalanges: the ridges run transversely across the finger at the joint, radially at the sides of the field, and tangentially over the top of the finger. This describes a boundary with two gates (Fig. 9a).

The boundary index here is 0. The theorem tells us that within this subfield each loop will have a compensating triradius and each whorl, two.

A second advantage is the elimination of apparent anomolies. For example, to continue with the distal phalange; exceptionally, a condition known as anonychia arises in which the nail is missing (Penrose, 1965). As a result the radial orientation of the ridges at the boundary is continued over the top of the digit to provide a boundary to the distal phalange sub-field with only a single gate. The index theorem correctly predicts an unpaired loop whereas one must modify Penrose' formula to count nails instead of digits. This modification is of no avail however in the case of the clinical anomaly called "ridges-off-the-end" syndrome (David 1971) where the ridges run radially off the fingertips

in the presence of a nail. Furthermore there is also the anomaly of a deficient triradius in the absence of an extra digit, correlated with a tangential zone on the thenar region of the palmar boundary, that is to say an extra gate on the boundary in the absence of an extra digit (Penrose, 1965). All these oddities cease to be anomolous in the light of the index theorem.

It appears therefore that it is neither the number of digits, nor the number of nails that is the fundamental parameter accounting for packing, but the number of gates on the boundary. Furthermore in the case of severly malformed hands and feet, it is likely to be easier and more reliable to assess the number of gates on the boundary directly than to worry over digits and the complication of the presence or absence of nails. In addition, the index theorem in the mathematical setting of the singularities in two-dimensional, non-oriented vector fields (see appendix) offers deep insights into the nature of the packing of dermatoglyphic fields, and permits formal comparison with other biological systems.

## Discussion

How is the pattern developing within a mass culture of fibroblasts or on the surface of an embryonic hand to be described and accounted for?

The fibroblast system is patterned by discontinuities in a sheet. Even though cells make up the system, the pattern cannot be wholly accounted for in cellular terms. First as we discussed in the introduction, the scale of discontinuities is large in comparison with cell size. Second, because pattern does not stem from different cells within the system taking distinct developmental pathways like those that would produce spots on a leopard skin: the system is made up of interchangeable elements. Furthermore, while important aspects of pattern develop autonomously and locally and may be explained in terms of cell behaviour, to a large extent, local detail reflects the operation of global packing constraints. This global-to-local influence is not easily dealt with in terms of cellular behaviour alone, and there is no biological language to carry the discussion further.

A larger format is required, and the elaboration of an appropriate model is our aim.

## The Model

Both patterns studied are composed of close-packed linear flexible elements – motile fibroblasts, and non-motile stringlike dermal ridges. Neither system is characterised by a repeating pattern, as on a wallpaper, appropriately modelled using Euclidean geometry. Instead, the formal elements are invariant under plastic deformations, as well as rigid motions, and thus require a topological modelling. For this reason the elements are modelled by vectors in a vector field. The vector field is an appropriate format for modelling the qualitative aspects of pattern in a manner that permits quantitative measurements to be

made using the topological index. In both systems the elements pack side by side on a two-dimensional surface and, in the case of fibroblasts, under the known constraints of contact guidance (Weiss, 1961) and contact inhibition (Abercrombie, 1967), the model, therefore, employs a two-dimensional vector field. There is no evidence that fibroblasts or dermal ridges possess specific front and back poles; vectors, therefore, whose sole difference is a 180° difference in orientation, are identified (or made equivalent) to give a non-oriented vector field or line field. Both patterns are characterised by smooth change around point discontinuities confirming that the vector field be taken as smooth or differentiable. The model arrived at is a smooth, planar, non-oriented vector field.

The topology of this field allows for only three nondecomposable singularities, (mathematical analogs of discontinuities) corresponding to the observed discontinuities of index 0 (parallel array), and indices $+^1/_2$, and $-^1/_2$. The topology also includes other decomposable singularities, whose indices are integral multiples of $^1/_2$, including those corresponding to the unstable $+1$ and $-1$ discontinuities observed.

The index theorem quantitates the additive nature of rotations in the vector field, in the vector field, and we have demonstrated corresponding behaviour in our two biological systems.

*Global Constraints and Implications of the Model*

The topological model applies to a confluent close-packed fibroblast culture, it does not apply to a sparse culture. Consider the difference between these two situations.

Prior to confluence the cells behave largely independently of their neighbours or form small, local autonomous associations little influenced from without. Only a limited degree of order arises. Inherent in the multicellular system, mutual cellular influences assume increasing importance as close-packing is approached. After confluence, the entire culture close-packed, mutual influence is at its most restrictive, and a higher degree of order results therefrom.

With the creation of a unitary, close-packed field, constraints arise that cannot be assigned to one sub-compartment of the field and not to another, constraints therefore which can be described and quantitated only in terms of the whole. Such we term global constraints, and they derive essentially from mutual influence and not from new behaviour on the part of the cells.

The purpose of the model is to deal quantitatively with global constraints.

A three-gated field, to take an example, must have at least one internal branch point. The model implies that the "cause" of the branch point is the topology of the close-packed field, and is not to be located in some special feature of the elements in the region where the branch point forms. Similarly, the four principal triradii on the normal hand are a consequence of the six gated boundary.

Notice that whereas explanation in biology often involves a mapping of variation in one level of organisation to something else varying in a lower

level, seen as the cause, in contrast, the interrelations of the parts *are* the cause here, and the phenomenon is not reduced.

A topological analysis does not account for all aspects of pattern; it does not account for the absolute number and locations of discontinuities in a field, only their relative balance. By way of illustration consider again the distal phalange sub-field. The boundary index is 0. The normal phalange presents either an arch, or a loop and one triradius, or a whorl and two triradii. All three possibilities are consistent with the index theorem. Which one is realised in a particular case, depends upon variables in the developmental system; thus, it is believed that a flat contouring of the digital surface around the time the pattern is becoming established favours the arch, and a pronounced bulging, the whorl.

The smaller the field, the more restrictive are the constraints formalised under the index theorem; for this reason the theorem virtually predicts pattern in small bounded fields. With this in mind, it is possible to envisage how boundary constraints could determine the reliable development of a simple pattern in young organ rudiments. It is interesting that the size of young organ rudiments (1 mm) is about the same as the diameter of our small bounded fields illustrated. Would it not be unparsimonious of the embryo not to make use of the ordering potential offered by boundaries? In the case of the dermatoglyphic field we know that the boundary dispositions are established first and the ridges develop from the periphery inwards.

Cell packing under global constraints is a mindless affair although the overall system may be complex. The model suggests that on the basis of very general properties of the elements, the system achieves a high degree of organisation and entrainment without demanding much from the complex apparatus of the cell.

## Informal Mathematical Appendix

The model we shall adopt to describe pattern in a mature fibroblast culture and of dermatoglyphics is a variant of a vector field in a planar region. As an element is a bipolar spindle (either a fibroblast or a dermal ridge) with position and orientation it can be identified with a line segment or vector. However, there is no "structure" to warrant distinguishing between vectors of equal length originating from the same point and on the same line but pointing in opposite directions. Therefore the vectors v and $-v$ are identified. The resulting non-oriented vector field or line field is a rule which assigns to each point such a pair of vectors. Wherever possible, neighbouring elements lie parallel and the entire system is characterised by smooth change and demonstrates coherent behaviour. The vector field is therefore taken to be smooth or differentiable. This implies that given the equations describing the vector field in a neighbourhood of a point, the derivatives of all orders will be continuous.

## Topological Index

The topological index provides information about properties of a vector field which remain invariant under plastic deformations accompanying growth and evolution of the field over time. In the case of the simplest field in which all line segments share a common direction (parallel array) the index is everywhere zero. In other cases there will be singular points in the field where the vector is zero. These singularities are the mathematical analogue of the discontinuities observed in fibroblast cultures. The index around singularities takes on non-zero values.

## Computation of the Index

We compute the index of a field F about a curve J. J, also called a circuit or Jordan curve, is a simple, closed, non-self-intersecting curve that passes through no singularities of the field F. Choose a sufficiently large number of sample points around the curve and sum the angular differences between successive vectors in the course of describing one complete rotation of the curve. Divide the sum by $2\pi$. Where the field rotates in the same direction as the circle is toured the sense of rotation is taken as positive, otherwise it is taken as negative. In the following examples we consider the indices of the five singularities relevant to this study, and how the sign convention operates.

*Example 1* (Fig. 11): Trivial Case: The parallel array. All vectors pointing the same way means no angular differences between them. Index 0.

*Example 2 (Fig. 12)*: Radially disposed elements about a singularity (a), Diagram (b) indicates the direction of the vectors on the curve J. As a clockwise tour of J is made the field rotates through $2\pi$ radians, also clockwise. In Fig. c these vectors are redrawn originating from the same point but without change of slope, in order to make plain the sense of rotation of the field (compare with Figure 13c where the rotation is in the opposite sense). Index equals $+1$.

*Example 3 (Fig. 13)*: This figure combines features of the two previous examples. In the upper semicircle the field rotates through $\pi$; the lower semi-circle lies within a parallel array. Index $+{}^1/_2$.

*Example 4 (Fig. 14)*: Singularity at the confluence of Four Arrays. Diagram (b) shows the field intersecting J. As the clockwise tour of J is made, the field rotates counter clockwise see diagram (c). The total variation is $2\pi$. Hence Index $= -1$. Therefore, by convention, the rotation is taken as negative.

*Example 5 (Fig. 15)*: This singularity combines examples 1 and 4 and Index $= -{}^1/_2$.

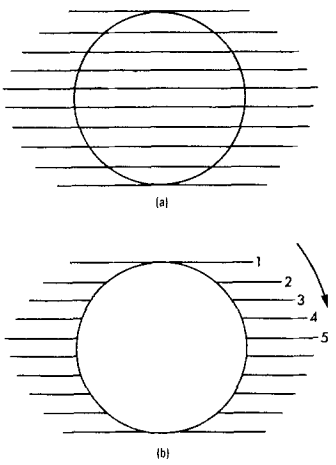


Fig. 11a–b. Example 1

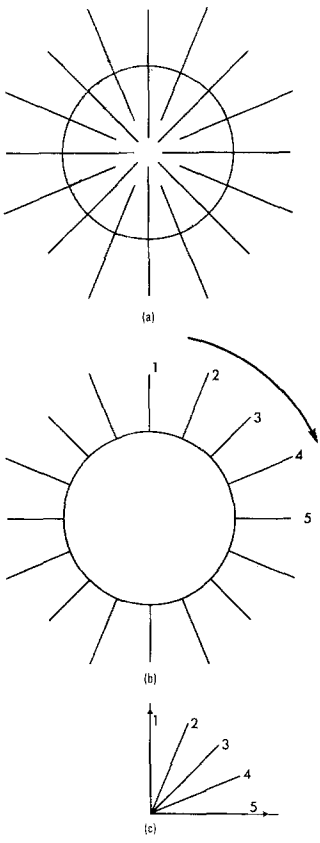


Fig. 12a–c. Example 2

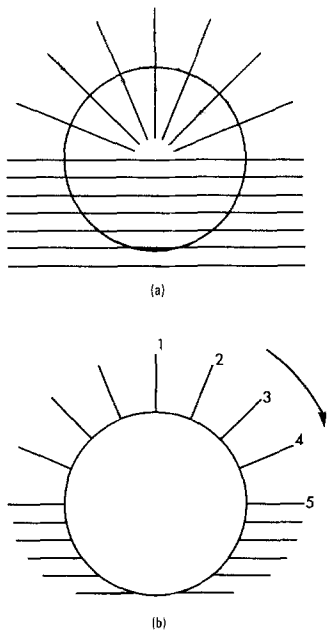


Fig. 13a–b. Example 3

*Formal Definition* (Lefschetz, 1957; Petrovski, 1966) Where the field F is given by the ordered pair of real valued functions X and Y,

F = X(x,y), Y(x,y) then the *index* of
F around the circuit J, I(F,J) is given by the
line integral

$$\frac{1}{2\pi}\oint \frac{XdY - YdX}{X^2+Y^2}.$$

Where the curve encloses just one singularity, the index can be said to characterise the singularity. Hence the figures observed in fibroblast cultures corresponding to example 3a (Fig. 13a) are referred to as "$+^1/_2$ discontinuities".

*The Index as a Topological Invariant of the Vector Field*

There is no way by which a singularity can be continuously deformed into another of a different index: two singularities of different index are topologically

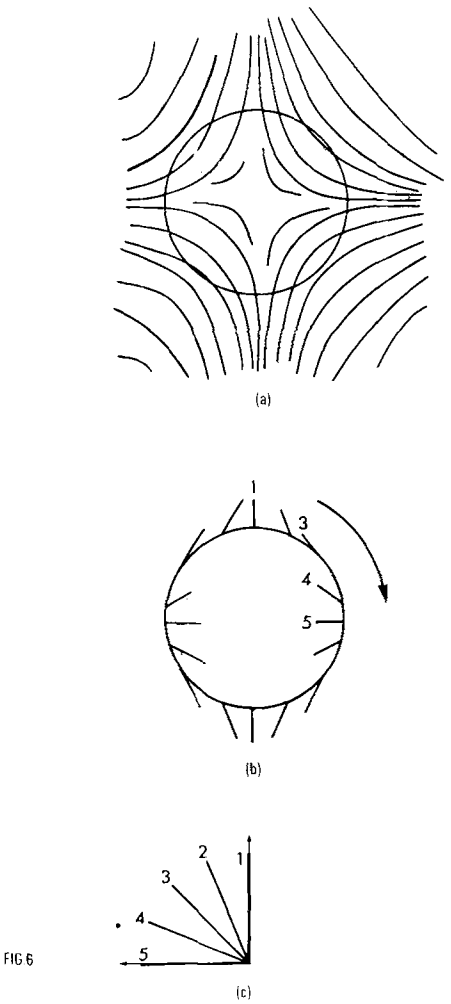


**Fig. 14a–c.** Example 4

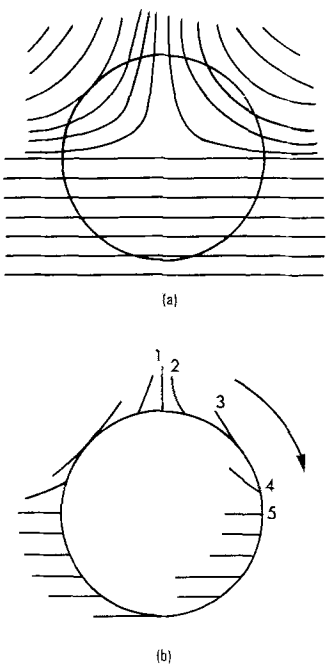


**Fig 15a–b.** Example 5

distinct. The index associated with a singularity is not altered under continuous deformations and orthogonal transformation. Certain orthogonal transformations may be arrived at by continuous deformations.

The index helps one to appreciate complementarity relations:

$$(+{}^1/_2)+(-{}^1/_2)\rightarrow 0.$$

This means that a field or sub-field containing just one $+{}^1/_2$ and one $-{}^1/_2$ singularity can be continuously deformed into a field containing no singularities. (The directed arrow is used instead of an equal sign to indicate that the change can only go in one direction—the inverse change is a *discontinuous* deformation. The simplification of the fibroblast pattern resulting from the elimination of discontinuities and the stability of the large arrays so formed, provides further validation of the differentiable vector field model).

Notice that the mathematics only restricts or describes what may occur, it does not guarantee that it will occur in a fibroblast culture.

*The Index Theorem*

The theorem provides the basis for quantifying the global constraints "forcing" local behaviour. As motivation, two simple theorems are stated and their implications considered.

*Theorem 1.* If two circuits, J and $J^1$ enclose the same singularities of the field F, then the index I of F computed around each is the same.

$$I(F,J)=I(F,J^1).$$

This means that the result does not depend on the choice of curve, only on the enclosed singularities. There is a further additive property of indices. Consider three circuits, J, $J_1$ and $J_2$. $J_1$ and $J_2$ enclose non-overlapping regions of the field, each containing singularities, with J completely surrounding them both without capturing additional singularities (Fig. 16).

*Theorem 2.* The index of F around J equals the sum of the indices around $J^1$ and $J^2$. Or if $J=J_1+J_2$, then,

$$I(F,J)=I(F,J_1)+I(F,J_2).$$

We extend the last result. Let $\Omega$ be a planar region where the vector field F is defined and whose boundary is a circuit J not passing through singularities of F. Each singularity in $\Omega$ es enclosed in a small closed curve and the index computed. The curves can be chosen so that they do not overlap. J captures no additional singularities. Theorem 2 is applied.

*Theorem 3* (Index). The sum of the indices of the singularities of a vector field F contained within a planar region bounded by a circuit J equals the index of the field F around J. Where the boundary J is defined in advance as in the experiments described, the balance of singularities of each sign is determined by the index of F on J.

Where J encloses a random set of singularities, the sum of their indices determines the index of J.

*Boundary Index and Gates*

The radial field resulting from a template of radial scratches rotates through 2 radians, giving a boundary index of +1. The boundary index can be changed by the introduction of "gates".

*Example (Fig. 17)*: Consider the situation where half of the radial template (A) is replaced by a tangential line or gate (B). The cells plated onto this

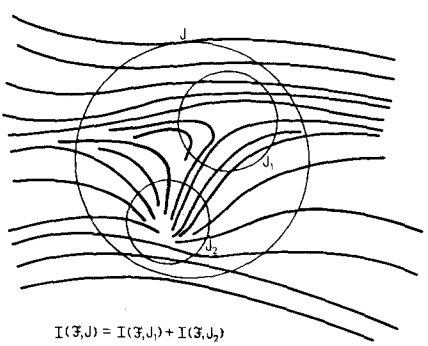


Fig. 16. Theoremz (see text)

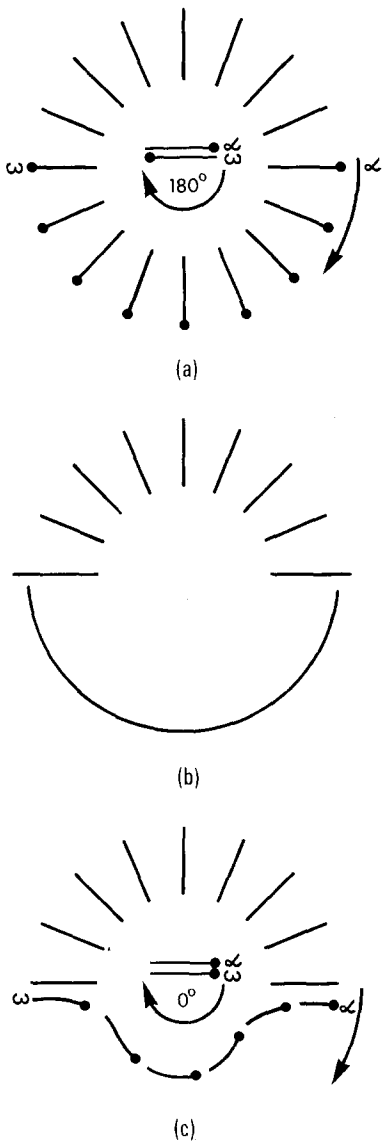


Fig. 17a–c. See text

field will be smoothly contoured around the transition points. It is this field (C) we wish to measure, not the template and here the transition from radial to tangential is continuous.

Compare the amount of angular rotation in the lower semicircles of (A) and (C). In A the field goes through $\pi$ radians while in C there is zero net rotation. In this example the gate has reduced the angular rotation by $\pi$. The upper halves are identical, therefore the index around the curve $C = {}^1/_2$.

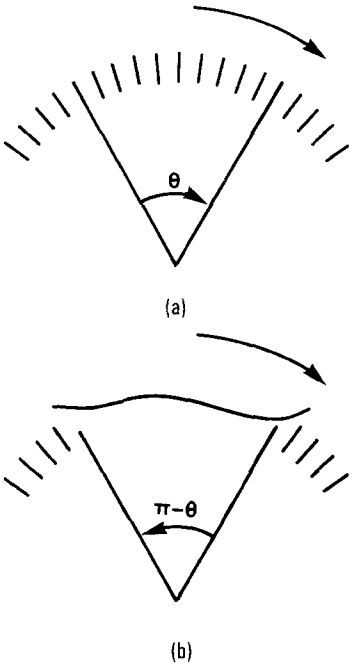


Fig. 18a–b. See text

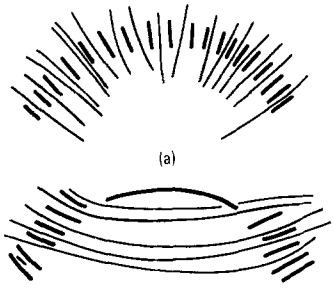


Fig. 19a–b. See text

This is also true more generally. Each gate on the boundary will reduce the net rotation by $\pi$. Compare these two boundary arcs—(Fig. 18) one from a radial field and the other where a portion has been replaced by a gate.

In Figure (a) the field describes a rotation through $\theta$. The rotation in Figure (b) proceeds in the opposite direction and the amount is $-(\pi-\theta)$. The difference $-(\pi-\theta) \; -\theta$ is $-\pi$. Notice that the difference is independent of the size of $\theta$, hence the size of the gate. Notice the kind of change in the field that results (Fig. 19). This is equivalent to the removal of the occasion for one $+{}^1/_2$ discontinuity.

To summarise, if the boundary has n gates, the amount of rotatio is $(2\pi - n\pi)$. Dividing by $2\pi$ for the index gives the simple formula:

$$\text{BOUNDARY INDEX} = 1 - {}^1/_2 \text{ (NUMBER OF GATES)}$$

Each gate reduces the boundary index by ${}^1/_2$.

We would like to thank the Cancer Research Campaign for financial support of one of the authors (F.W.), E.C. Zeeman for his suggestion that the topological index be used in analysing fibroblast pattern, and our colleague, Jonathan Bard, for most useful criticisms and discussions. We are grateful to Ian Waddell, Norman Davidson and Sandy Bruce for graphics and to Elaine Troup for manuscript preparation.

## References

Abercrombie, M.: Contact Inhibiton: The phenomenon and its biological implications. Nat. Canc. Inst. Monogr. **26**, 249–277 (1967)

Cummins, H., Midlo, C.: Fingerprints, Palms and Soles: an Introduction, Dover Publications, New York (1961)
David, T.J.: Ridges off the end—a dermatoglyphic syndrome. Hum. Hered. **21**, 39–53 (1971)
Elsdale, T.R.: Parallel orientation of fibroblasts in vitro. Exp. Cell Res. **51**, 439–450 (1968)
Elsdale, T.: Pattern formation in fibroblast cultures, an inherently precise morphogenetics process. Towards a Theoretical Biology, (G.H. Waddington, ed.), Edinburgh University Press, **4**, 95–108 (1972)
Elsdale, T.: The generation and maintenance of parallel arrays in cultures of diploid fibroblasts. Biology of Fibroblast (E. Kurlonen and J. Pikkarainen, eds.), Academic Press, London, 41–58 (1973)
Elsdale, T., J. Bard.: Cellular interactions in mass cultures of human diploid fibroblasts. Nature **236**, 152–155 (1972)
Hamilton, L.: The formation of somites in *Xenopus*. J. Embryol. Exp. Morph. **22**, 253–264 (1969)
Lefschetz, S.: Differential Equations: Geometric Theory, Interscience, New York (1957)
Penrose, L.S.: Dermatoglyphic topology. Nature **205**, 544–546 (1965)
Petrovski, I.G.: Ordinary Differential Equations (tanslated by Silverman, R.A.) Dover Publications, New York (1966)
Weiss, P.: Guiding principles in cell locomotion and cell aggregation. Exp. Cell Res. Suppl. **8**, 200–281 (1961)

*Received January 21, 1976*
*Accepted in revised form May 5, 1976*

# Addendum in proof

Zum Beitrag Tom Elsdale and Frances Wasoff, Fibroblast Cultures and Dermatoglyphics: The Topology of Two Planar Patterns, S. 121–147.

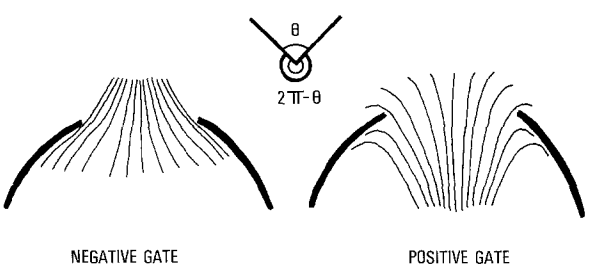


Whereas we have considered in this paper only gates on the boundary that reduce the boundary index by $^1/_2$ (negative gates), positive gates increasing the boundary index by $^1/_2$ can also arise. A gate of this latter type is responsible for the dermatoglyphic anomaly dealt with on page 138. The difference between the two types of gate is a matter of the convergence of the tangential alignments. The alignments converge externally in the case of a negative gate and internally in the case of a positive gate, as illustrated in the accompanying figure. The rotation about the negative is $\theta$, that around the positive gate $2\pi-\theta$. Only negative gates are seen in fibroblast cultures because the cells are reluctant to bend and preferentially take the straighter course.